Research Article

Mengya Ye, Jiahui Pan, Zhan Guo, Xiaoyu Liu, and Yu Chen*

Effect of ball milling process on the photocatalytic performance of CdS/TiO_2 composite

https://doi.org/10.1515/ntrev-2020-0045
received April 18, 2020; accepted May 11, 2020

Abstract: CdS/TiO_2 composite photocatalysts were made by the method of secondary ball milling at different ball milling speeds, milling time, and material ratios. After the secondary ball milling process, parts of the samples were calcined at high temperatures. X-ray diffraction (XRD) and UV-Vis diffuse reflectance spectroscopy (DRS) were used to observe the powder particle size, structural defect, bandgap, and absorption spectrum of the samples. Combined with the observation results, the effects of ball milling speed, time, material ratio, and high-temperature calcination on the photocatalytic performance of CdS/TiO_2 composite samples were analyzed. Furthermore, the methyl orange (MO) was chosen to simulate pollutants, and the photocatalytic degradation rate of CdS/TiO_2 composite photocatalysts for MO was evaluated under sunlight and UV irradiation conditions. The photocatalytic degradation efficiency of CdS/TiO_2 photocatalyst under UV irradiation is much higher than that under sunlight irradiation. The experimental results reveal that secondary ball milling can effectively promote the formation of CdS/TiO_2 composite nanostructure and the high-temperature calcination can reduce the bandgap width, which makes the samples easier to be excited. When the ball milling speed, time, and material ratio were respectively 400 rpm, 10 h, 25:75, and then calcined at high temperature, after 2 h of irradiation under UV light, CdS/TiO_2 composite photocatalysts exhibited maximum photocatalytic degradation efficiency of 57.84%.

* **Corresponding author: Yu Chen,** College of Civil Engineering, Fuzhou University, Fuzhou 350116, China, e-mail: kinkingingin@163.com, tel: +86 18030219629
Mengya Ye, Zhan Guo: College of Civil Engineering, Fuzhou University, Fuzhou 350116, China
Jiahui Pan: CSCEC Strait Construction and Development Co., Ltd, Fuzhou 350015, China
Xiaoyu Liu: School of Urban Construction, Yangtze University, Jingzhou 434023, China

Keywords: CdS/TiO_2, photocatalysis, ball milling process, irradiation condition, high-temperature calcination, methyl orange solution

1 Introduction

Nowadays, with the speedy development of the economy and increasing awareness of environmental protection, people pay more and more attention to the utilization of solar energy and photocatalytic treatment of organic pollutants by semiconductors [1]. Photocatalysis technology has been considered as one of the most efficient solutions to address air pollutants due to its preferable properties and complete degradation [2–4]. Among ZnO [5], CeO_2, TiO_2, etc, TiO_2 has been the preferred photocatalyst on account of its excellent photocatalytic performance, environmental protection, stable chemical properties [6,7], inexpensiveness, nontoxicity, and long service life [8,9]. In particular, when compared with the traditional methods, it is of great significance to the degradation of pollutants in wastes and can even completely degrade pollutants in sewage [10,11]. Therefore, TiO_2 has been used in extensive variety of applications, such as optics, self-cleaning, water splitting, catalysts, electrical porcelain [12,13], reducing environmental pollution [14], and other aspects [15–17], which has prompted many people to use various methods, such as microwave-assisted solvent heat method and ion exchange method to prepare TiO_2 [18,19]. For example, Maruthapandi et al. [20] presented polyaniline composite formed with TiO_2; SiO_2 is an effective adsorbent for the degradation of the organic contaminant in water, and the adsorbed contaminant can be desorbed to achieve reuse. Zangeneh et al. [21] used L-histidine with TiO_2/CdS photocatalytic nanocomposite materials to prepare a polyethersulfone membrane. The results showed that due to the addition of them, the surface roughness of the membrane had a good change and its porosity and

hydrophilic energy were also improved, thus improving the antifouling performance, which is of great significance to the protection of water resources. In addition, activated carbon nanocomposites synthesized with TiO_2 and other substances have been used to remove airborne pollutants such as xylene [22,23]. In 2020, Rambabu et al. [24] proposed a tricomponent photocatalyst consisting of TiO_2 multileg nanotubes, CdS nanoparticles, and reduced graphene oxide, which has good light absorption performance and can efficiently generate easily separated carriers under light irradiation. Furthermore, TiO_2 was modified with Cu(OH)(2) as a catalyst to make composite catalyst and used it for photocatalytic hydrogen production, which shows a great hydrogen yield [25], and Qin et al. [26] reached a similar conclusion through experiments. However, since TiO_2 with a wide bandgap width of 3.2 eV, especially the crystalline phase of anatase can merely be excited under UV light, resulting in about 50% visible light cannot be utilized. At the same time, some of the electron-hole pairs induced by UV are easy to recombine, which greatly limits its photocatalytic performance [27,28].

In recent years, more in-depth studies have been conducted at home and abroad, to conquer these defects of TiO_2 mentioned earlier and improve its photocatalytic activity. A large number of studies have shown that modification methods such as ion doping, semiconductor compounding, noble metal deposition, and photosensitization can extend the optical photoabsorption wavelength of pure titanium dioxide to the visible light range and enhanced its catalytic activity to different degrees [29,30]. Trejo-Tzab et al. [31] proposed that the photocatalytic activity of TiO_2 can get improvement by nitrogen (N_2) doping and deposition of Cu nanoparticles, the degradation rate of MB solution was used to evaluate the photocatalytic activity of this improved TiO_2. The experimental phenomenon indicated that under the condition of low-intensity gas plasma, incorporating Cu into TiO_2 P25 to obtain nitrogen-doped TiO_2/Cu had higher photocatalytic activity than pure anatase TiO_2. Also, Tokmakci et al. [32] proved that the photocatalytic performance of titanium dioxide photocatalysts mixed with both boron (B) and zirconium (Zr) is higher than that of single element mixed TiO_2 and pure anatase TiO_2. This kind of phenomenon can attribute to the reduction in the size of the photocatalyst and the successful weaving of B and Zr into the crystal structure by the mechanical ball milling method. Similarly, the sulfur (S)-doped TiO_2 photocatalysts newly designed by Jalalah et al. [33] extended their absorption edge to the visible light range via incorporating sulfur into the lattice structure of TiO_2, revealing an excellent photocatalytic activity of the new photocatalysts to MB in the visible region. Petrovic et al. [34] synthesized TiO_2/CeO_2 photocatalyst by high energy ball milling method. According to the degradation efficiency for MO solution, one could see that TiO_2/CeO_2 composite material had higher photocatalytic activity than anatase TiO_2, resulting from the effective separation of electron/hole pairs on TiO_2 because of the addition of CeO_2. Aysin et al. [35] prepared silver-loaded TiO_2 photocatalyst, the number of photogenerated charge carriers involved in the degradation process greatly increased because of the introduction of Ag and gave rise to the improvement of photocatalytic activity. Even with very little Ag loading, the photocatalytic degradation efficiency for MO of the silver-loaded samples was 50% higher than that of the unloaded TiO_2 after 1 h of irradiation under UV light. Chen et al. [36] obtained TiN/TiO_2 composite nanoscale photocatalyst by ball milling of TiO_2 in TiN-doped aqueous solution, and when compared with pure anatase TiO_2, TiN/TiO_2 composite nanoscale photocatalyst has better photocatalytic performance under both sunlight and ultraviolet light irradiation. The enhancement in the photocatalytic performance of the TiN/TiO_2 may well owe to the extension of photoabsorption wavelength of the photocatalyst and the raise of the Ti^{3+} reaction center on the surface. Moreover, Balakrishnan et al. [37] used methylene blue to simulate pollutants to investigate the photocatalytic performance of TiO_2–ZnO nanostructures. The result proves that TiO_2–ZnO nanostructures had good photocatalytic performance in both visible and ultraviolet light. Habib et al. [38] also conducted an in-depth study on the photocatalysis of TiO_2–ZnO nanocomposites.

It can be seen from the studies listed above that in recent years, although some effects have been achieved through the modification of TiO_2, most modification methods are difficult to be applied and industrialized due to high preparation cost, complicated process, and limited performance improvement. In 2015, Zhou et al. [39] prepared CdS/TiO_2 composite photocatalytic material by a simple mechanistic method to boost the photocatalytic activity of TiO_2 by sensitization and surface hybridization of CdS. In the paper, CdS/TiO_2 samples were made by similar mechanochemical secondary ball milling process (dry ball milling and wet ball milling), to explore the optimal ball milling process and the effect of high-temperature calcination on the photocatalytic performance of CdS/TiO_2 composite photocatalyst produced by secondary ball milling process; methyl orange (MO) was used to simulate pollutants, and the photocatalytic activity of CdS/TiO_2 composite photocatalyst was analyzed by UV-Vis diffuse reflectance

spectroscopy (DRS) and X-ray diffraction (XRD). CdS is a kind of commonly used photosensitive resistor, which has a strong photoelectric effect on visible light. The bandgap width of it is relatively narrow, and the spectral response range is close to that of visible light. However, electron holes have strong redox ability and can oxidize S^{2-} on the surface under light irradiation, resulting in severe photocorrosion in the use of CdS alone. After the combination of TiO_2 and CdS with a large difference in bandgap width, electrons can transition within the visible region, leading to the high-efficiency separation of electron holes. Therefore, TiO_2 can be excited in the visible range, and the photogenic holes of CdS can be neutralized, which can inhibit the photocorrosion phenomenon and enhance the photocatalytic performance of CdS/TiO_2, thus achieving more efficient degradation of pollutants in water. Although there have been many solutions for organic pollutants in water, for example, Yi et al. [4] studied the adsorption performance of silica gel to organic pollutants in water but only at low concentrations of pollutants. The production method is complex and has strict requirements on precision and time, which is not suitable for large-scale production or industrial utilization.

2 Experiment

2.1 Materials and methods

The materials used in this experiment are nanoscale pure anatase titanium dioxide (TiO_2, if used as an industrial application, Wang et al. [19] proposed large-scale synthesis of high purity TiO_2 by ion-exchange method, cadmium sulfide (CdS) and MO, all of which are analytical pure drugs produced by China National Pharmaceutical Corporation.

CdS/TiO_2 composite photocatalysts were made by the secondary balling milling method, which was carried out in two steps. The first step was to fully compound the raw materials evenly mixed by dry ball milling, and the second step was to refine the particle size of powders by wet ball milling. The detailed preparation processes of CdS/TiO_2 composite photocatalysts are as follows: (1) according to the designed material ratios (i.e., the mass ratio of CdS to TiO_2), the TiO_2 and CdS powders were accurately weighed and added into the corundum ball mill tanks in turn. Corundum balls with diameters of 10, 5, and 2.5 mm and a mass ratio of 1:3:6 with a total mass of 200 g were selected for grinding ball beads. The mass ratio of corundum balls and materials was 20:1. Place the ball mill tanks in the ball mill after the ingredients are finished. (2) On the basis of ball milling speed and ball milling time designed in the experiment, the TiO_2 and CdS powders were ground by dry ball milling. (3) After the completion of dry ball milling, anhydrous ethanol was added to make the mixed materials show sticky shape and then put it into the ball mill again with the same milling parameters for wet ball milling for 2 h. (4) After the ball milling was finished, the products were collected immediately, then dried and put into the resistance furnace to calcine at 400°C for 2 h. (5) The materials prepared by the above processes were fully ground for 30 min to make the samples.

2.2 Characterization

The properties and structures of the samples were characterized by UV-Vis DRS and XRD (Cu Kα, scanning rate was 4°/min, and the transport current and acceleration voltage. Respectively. were 40 mA and 45 kV). Based on the above analyses, the XRD patterns of the CdS/TiO_2 composite photocatalysts and the average particle sizes were obtained. Moreover, the absorbance spectrum of the photocatalysts was acquired by utilizing the UV-Vis spectrophotometer (type LAMBDA 650), and the band gaps as well as the light absorption capacity were further analyzed.

2.3 Test of photocatalytic performance

MO is a common organic dye, which has no volatilization and is difficult to decompose and oxidize under light and can be used to simulate experimental contaminants. In this experiment, MO simulating pollutants were utilized to study the photocatalytic properties of CdS/TiO_2 composite photocatalysts, and the degradation rate was calculated by UV-2600 UV-Vis spectrophotometer. MO is a state of sodium sulfonate dyes, with the extension of photocatalysis time; MO was adsorbed on the surface of CdS/TiO_2 composite photocatalysts and eventually degraded to H_2O CO_2 and other inorganic substances. During the degradation, new substances appeared and the concentration of new substances was constantly increasing. However, due to the complexity of the products, limited test time, and instrument conditions, the intermediate products could not be completely separated.

UV-high-pressure mercury lamp and long-arc xenon lamp were used to simulate the environment of UV light

and sunlight irradiation conditions. The experimental procedures are as follows: (1) 10 mg/L mixture solution of MO was made by weighing a certain amount of MO and deionized water with a balance and a measuring tube, respectively. (2) Weighing 25 mg of photocatalyst with a balance and weighing 250 mL of MO solution with a measuring tube, both were placed in a container together, and 4 mL solution was removed by a pipette and put into the centrifuge tube in the opaque collection box. (3) The photocatalyst and MO mixed solution was put into the dark box and stirred with a magnetic stirrer for 30 min, then 4 mL solution was removed with a pipette and placed in the centrifuge tube in the opaque collection box. (4) Turn on the lamp needed for the experiment to preheat for 10 min. (5) The photocatalyst and MO mixture was irradiated with simulated UV light or sunlight for 2 h, while the cooling cycle was turned on. Place the solution directly under a light source so that it is fully illuminated and then stirred with a magnetic stirrer. Every 30 min, 4 mL of the solution was removed by a pipette and placed it in a centrifuge tube in the opaque collection box. (6) The samples of the solution collected in steps (3) and (5) were centrifuged in a centrifuge, and the supernatant liquor was removed with a pipette. The supernatant liquor was then centrifuged until the centrifuged solution did not precipitate. (7) Turn on the UV-2600 spectrophotometer and set its parameters. The centrifugal fluid collected from step (6) was poured into the colorimetric dishes, respectively, and the absorbance was measured (the absorbance of the centrifugal fluid was recorded as A_t according to the illumination time). After each measurement, the colorimetric dish was cleaned with deionized water. (8) In this experiment, the photocatalytic degradation efficiency (D) can be obtained by the following formula:

$$D = \frac{A_0 - A_t}{A_0} \times 100\%$$

where D is photocatalytic degradation efficiency, A_0 is the initial absorbance of the solution, and A_t is the final absorbance of the solution after t minutes of photocatalytic degradation.

3 Results and discussion

3.1 Photocatalysis mechanism

The CdS/TiO_2 composite photocatalyst prepared by the ball milling method has an effective composite structure. During the formation of the composite structure, CdS has a larger negative conductive potential and a smaller bandgap width than TiO_2, which results to the migration of the electrons (e^-) of CdS to the conductive band of TiO_2, achieving the purpose of e^- and holes (h^+) separation resulting in the enhancement of the photocatalytic capacity of CdS/TiO_2 samples.

When the composite photocatalyst is irradiated with light with energy greater than the bandgap energy of it, electrons are excited and enter the conduction band across the forbidden band, producing negatively charged highly active electrons (e^-) in the conduction band, leaving positively charged holes (h^+) in the valence band, thus producing highly active electron–hole pairs (h^+–e^-) on the surface of the photocatalyst. Under the action of an electric field, electrons and holes separate and migrate to the particle's surface. Holes on the surface of the composite photocatalyst can oxidize hydroxyl (OH^-) and water (H_2O) adsorbed on its surface to hydroxyl radicals ($HO^{\cdot}$), which is a kind of non-selective oxidant with strong oxidation capacity and can completely oxidize MO to CO_2, H_2O, and other inorganic substances.

3.2 Effect of material ratio on the photocatalytic performance

The material ratio is the ratio of raw materials needed to prepare unit products. This experiment prepared seven groups of CdS/TiO_2 samples with a material ratio of 10:90, 15:85, 20:80, 25:75, 30:70, 35:65, and 40:60, respectively, to explore the influence of different material ratios on the photocatalytic performance of CdS/TiO_2 composite photocatalysts. Under the conditions of ball milling speed of 400 rpm and ball milling time of 10 h, the photocatalytic performance of samples prepared with different material ratios was evaluated.

Figure 1 shows the photocatalytic degradation efficiency of CdS/TiO_2 composite photocatalysts that of different material ratios after 2 h of irradiation under UV light or sunlight. As can be seen from Figure 1 whose horizontal axis and the vertical axis, respectively, represent the material ratio and photocatalytic degradation efficiency of the samples, when the material ratio of CdS/TiO_2 composite photocatalysts is 25:75, the photocatalytic degradation efficiency is the highest, which is 8.04% and 54.32%, respectively, under sunlight and UV light. It follows that the photocatalytic performance of CdS/TiO_2 composite photocatalysts synthesized at a material ratio of 25:75 is higher than that of pure TiO_2, with photocatalytic degradation efficiency of 3.75% and

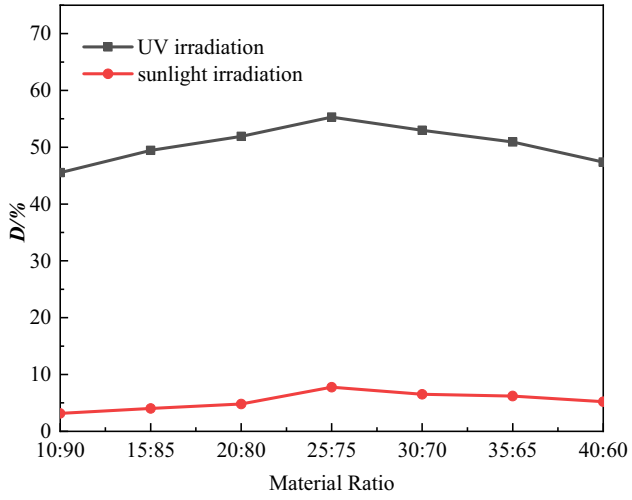

Figure 1: Photocatalytic degradation efficiency of CdS/TiO_2 composite photocatalysts with different material ratios.

49.04%, respectively, under the irradiation of sunlight and UV light. Figure 2 exhibits the UV-Vis diffuse reflectance spectra of the TiO_2 and CdS/TiO_2 composite photocatalysts. One can see that from the figure, when compared with pure TiO_2 (whose light absorption edge is at 390 nm in the ultraviolet light range), the absorption edge of CdS/TiO_2 composite photocatalyst after ball milling extends to the vicinity of 525 nm in the visible region, resulting in greatly enhancement of photocatalytic activity. Also, Figure 2 shows that the CdS/TiO_2 composite photocatalyst with a material ratio of 25:75 has the largest absorption spectral area, that is, the best photocatalytic performance, which is consistent with the data measured in Figure 1. The improvement of photocatalytic degradation efficiency can be put down to the effective composite structure of CdS/TiO_2 composite photocatalyst formed by ball milling under this material ratio. In addition, under the same conditions, the photocatalytic degradation efficiency of UV irradiation is much higher than that of sunlight irradiation, since the bandgap width reduces the utilization rate of sunlight. According to the XRD pattern shown in Figure 3, the characteristic diffraction peak value of TiO_2 and CdS still exist in the crystal phase of the CdS/TiO_2 composite photocatalysts after ball milling, and the decrease in crystallinity of the samples made by ball milling processes may be caused by the strain effect of lattice and the defects of lattice structure due to the action of mechanical force.

3.3 Effect of ball milling speed on the photocatalytic performance

The ball milling speed is the speed of the stirring shaft of the ball mill. Under the condition of low speed, medium speed, and high speed, the ball milling process can mix, compound, and crush the sample powders, respectively. As the speed of ball milling increases gradually, the ball milling energy will gradually increase and the composite will be more sufficient, but the damage to the material structure and the polymerization of the powders will also be more violent. To avoid the effect of the powder polymerization on the photocatalytic performance, dry ball milling was first used in this experiment, and then wet ball milling was carried out to refine the powder particle size. The photocatalytic properties of CdS/TiO_2

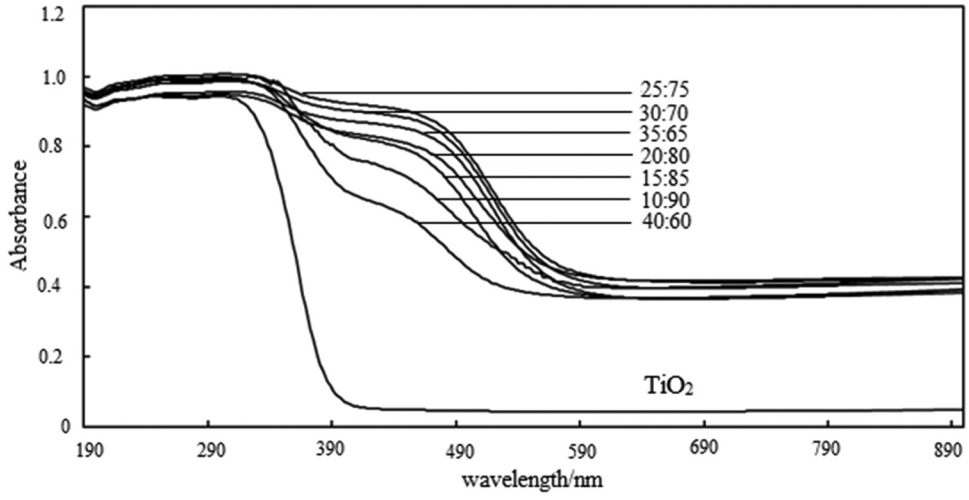

Figure 2: UV-Vis diffuse reflectance spectra of TiO_2 and CdS/TiO_2 composite photocatalysts.

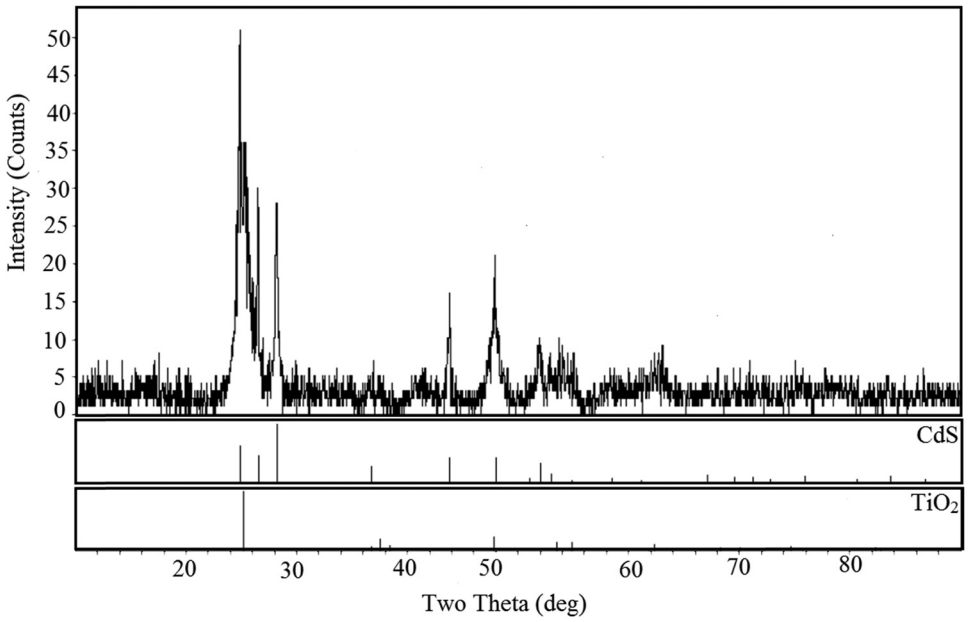

Figure 3: XRD pattern of CdS/TiO_2 composite photocatalysts with a material ratio of 25:75.

composite photocatalysts were evaluated at different ball milling speeds under the conditions of the preset material ratio of 25:75 and ball milling time of 10 h.

Figure 4 shows the photocatalytic degradation efficiency of CdS/TiO_2 composite photocatalysts exposed to UV light and sunlight for 2 h at different ball milling speeds. It is evident from Figure 4 that the speed of ball milling has an obvious effect on the photocatalytic performance of the samples, especially under UV irradiation. When the ball milling speed is no more than 400 rpm, the photocatalytic degradation efficiency of the CdS/TiO_2 composite photocatalysts exhibits a positive linear relationship with the ball milling speed, which may be due to the fact that the powders are not fully compounded, resulting in the low separation efficiency between holes and electrons; hence, the photocatalytic activity of the composite does not reach the maximum value. When the ball milling speed is 400 rpm, the CdS/TiO_2 composite photocatalyst has the highest photocatalytic degradation efficiency of 55.39%, indicating that the powders are most fully compounded and the composite structure has fewer defects under this ball milling speed. When the ball milling speed is higher than 400 rpm, a lot of adverse defects occur in the composite structure, which is not conducive to carrier separation and transfer resulting in the decrease of photocatalytic activity of the samples.

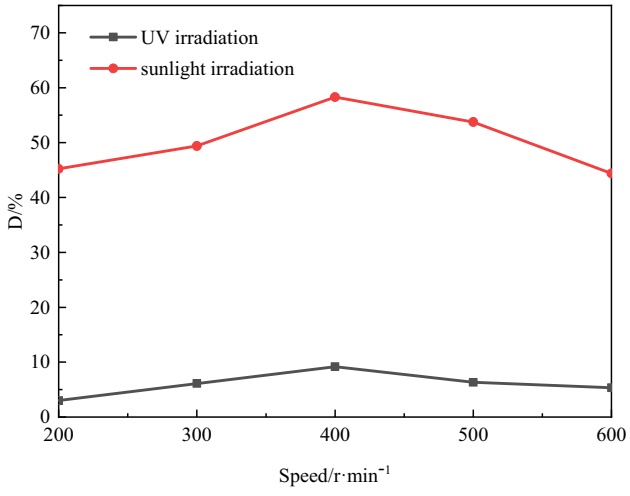

Figure 4: Photocatalytic degradation efficiency of CdS/TiO_2 composite photocatalysts with different ball milling speeds.

Moreover, Debye–Scherrer formula was employed to calculate the average particle sizes of CdS/TiO_2 composite photocatalysts prepared at different ball milling speeds, to explore the relationship between powder particle size and photocatalytic performance. Table 1 shows the detailed particle size of CdS/TiO_2 composite

Table 1: Particle size of CdS/TiO_2 composite photocatalysts at different ball milling speeds

Ball milling speed (rpm)	200	300	400	500	600
Maximum particle size (nm)	78.5	54.6	16.0	8.5	9.3
Average particle size (nm)	42.3	26.5	10.2	7.6	7.4

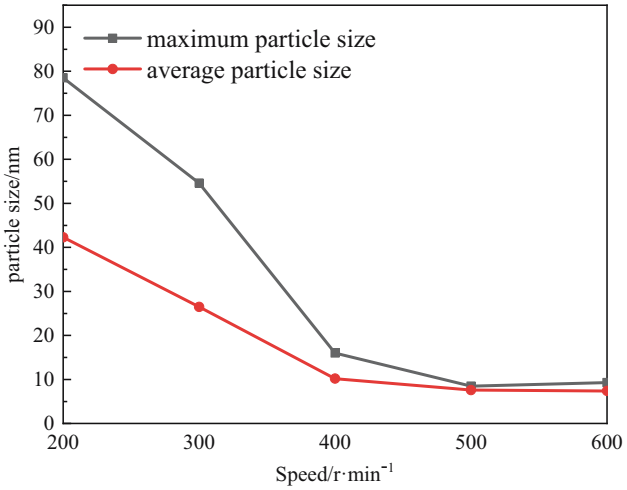

Figure 5: Particle size of CdS/TiO_2 composite photocatalysts at different ball milling speeds.

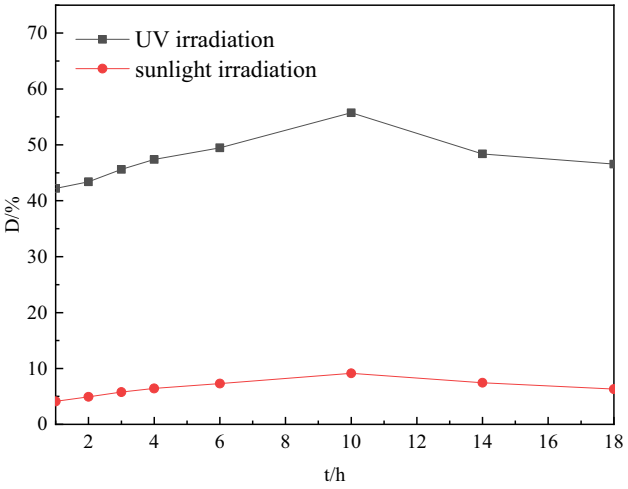

Figure 6: Photocatalytic degradation efficiency of CdS/TiO_2 composite photocatalysts at different ball milling time.

photocatalysts at different ball milling speeds. As the table indicates, with the gradual increasing ball milling speed, the average particle size of CdS/TiO_2 composite photocatalyst gradually decreases from 42.3 nm and finally stabilizes at about 7.4 nm. When the ball milling speed increases from 200 to 400 rpm, the average particle size of the sample decreases significantly by 32.1 nm, 75.9% compared with the average particle size at 200 rpm. However, when the ball milling speed increases from 400 r/min to 600 r/min, the particle size is reduced by only 2.8 mm. The photocatalytic degradation efficiency of CdS/TiO_2 composite photocatalyst is the highest at the ball milling speed of 400 rpm, corresponding to the nano-effect of nanoparticles and the trend of particle size reduction as shown in Figure 5.

3.4 Effect of ball milling time on the photocatalytic performance

The time of ball milling directly affects the particle size and purity of the product. During ball milling, due to the severe collision and friction of ball milling beads, part of the product will fall off. The longer of ball milling time, the more serious the pollution of the product will be. On the other hand, as mentioned above, with an increase in the ball milling time, the particle size of CdS/TiO_2 composite photocatalysts will gradually decrease to a certain value and tend to be stable, even if the ball milling time still increases. Under such a condition, the increase in the ball milling time will only lead to the contamination of the CdS/TiO_2 composite photocatalysts, but no longer improve the photocatalytic performance. Hence, one can see that finding the optimal ball milling time is quite crucial.

Under the conditions of the preset material ratio of 25:75 and ball milling speed of 400 rpm, Figure 6 shows the photocatalytic degradation efficiency of CdS/TiO_2 composite photocatalysts prepared at different milling time after 2 h of UV or sunlight irradiation. As is shown in the diagram, the photocatalytic degradation efficiency of CdS/TiO_2 composite photocatalyst with a ball milling time of 10 h is better than that of other ball milling time under both UV light and sunlight irradiation, so it can be considered that 10 h is the best ball milling time for preparing the CdS/TiO_2 composite photocatalysts. Similarly, Debye–Scherrer formula was also made use of calculating the average particle size of CdS/TiO_2 composite photocatalysts prepared under certain ball milling time, which is revealed in Table 2. The particle size of the sample significantly decreases when the ball milling time is no more than 10 h and gradually becomes stable after more than 10 h, which is consistent with the changing trend of the photocatalytic performance of the composite photocatalysts, which one can see from the comparison between Figures 6 and 7.

3.5 Effect of high-temperature calcination on the photocatalytic performance

To explore the influence of high-temperature calcination on the photocatalytic activity of CdS/TiO_2 photocatalysts (ball milling time of 10 h, i.e., optimal ball milling time) with different material ratios, the samples were put into a

Table 2: Particle size of CdS/TiO_2 composite photocatalysts at different ball milling time

Ball milling time (h)	1	2	3	4	6	10	14	18
Maximum particle size (nm)	87.4	62.6	45.2	34.9	23.3	16.0	10.6	9.4
Average particle size (nm)	63.3	46.9	25.8	16.5	12.9	10.2	8.5	7.8

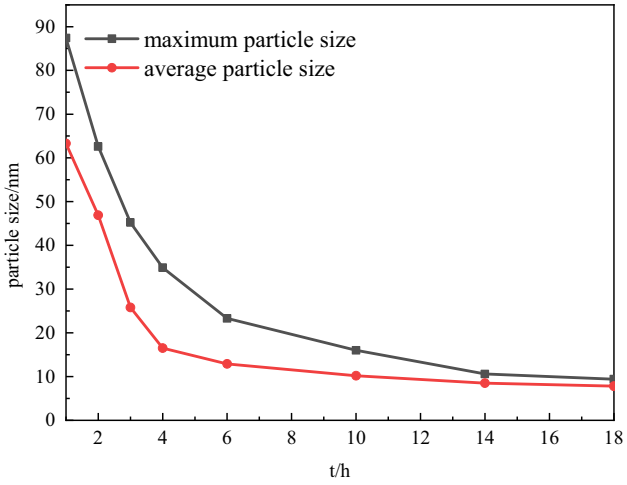

Figure 7: Particle size of CdS/TiO_2 composite photocatalysts at different ball milling time.

resistance furnace and calcined at 400°C for 2 h. Subsequently, the photocatalytic test was carried out under UV or sunlight irradiation for 2 h, and the calculated photocatalytic degradation efficiency was compared with that of the uncalcined samples, as shown in Figure 8. On the whole, the variation trend of photocatalytic degradation efficiency of CdS/TiO_2 photocatalysts with material ratio after calcination is approximately the same as that of uncalcined samples, but the photocatalytic degradation efficiency of calcined samples increases slightly, which may be owing to the reduction of adverse structural defects of CdS/TiO_2 composite photocatalysts. In addition, the bandgap width of the samples prepared and calcined under the optimal ball milling parameters and that of TiO_2 was calculated. As shown in Figure 9(a) and (b), the bandgap width of pure anatase TiO_2 is 3.05 eV, which is consistent with the research showing that the bandgap width of TiO_2 is 3.2 eV, while the bandgap width of CdS/TiO_2 composite photocatalyst is 1.88 eV. The wider the bandgap, the greater the energy required to excite the materials. In this experiment, the CdS/TiO_2 composite photocatalysts obtained by the secondary ball milling and calcining method have smaller bandgap width, easier excitation, and stronger photocatalytic performance.

4 Conclusions

In this paper, CdS/TiO_2 composite photocatalysts are made by the method of secondary ball milling, and the effects of material ratio, ball milling time, ball milling

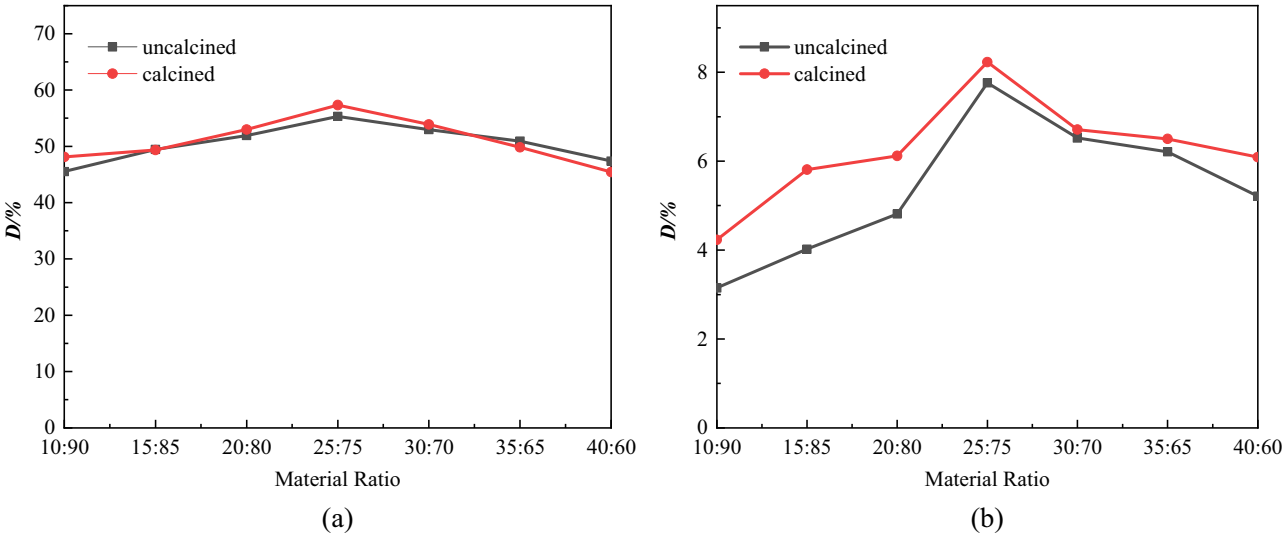

Figure 8: Photocatalytic degradation efficiency of calcined and uncalcined CdS/TiO_2 composite photocatalysts. (a) UV irradiation, (b) Sunlight irradiation.

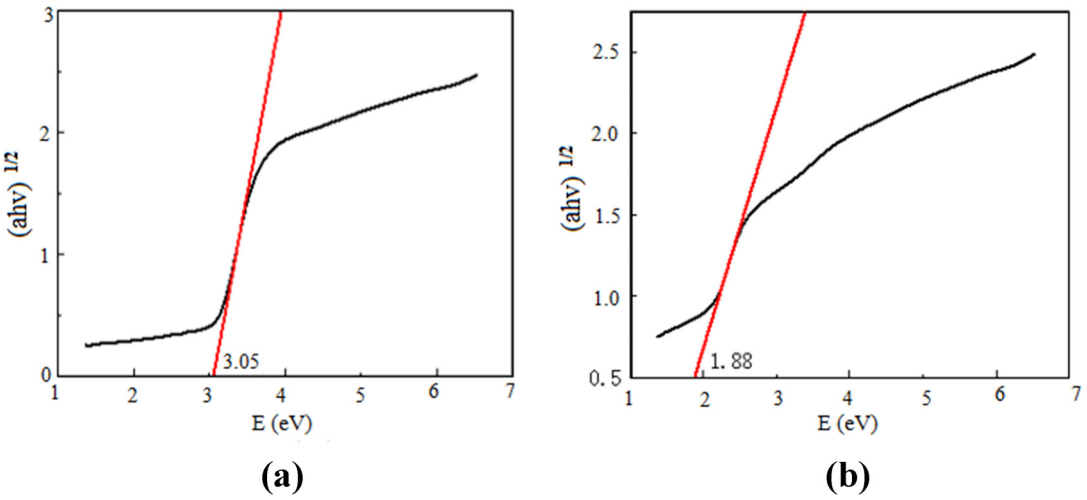

Figure 9: Band gap width of TiO_2 and CdS/TiO_2 composite photocatalysts. (a) TiO_2, (b) CdS/TiO_2.

speed, and high-temperature calcination on the photocatalytic performance are investigated. The following conclusions can be drawn from the experimental results:

1. The mechanochemical action of secondary ball milling can promote the dispersion of CdS on the surface of TiO_2 and the interaction between these two, forming an effective composite nanostructure with extended light absorption edge and small bandgap width, resulting in a significant improvement on the photocatalytic degradation rate of CdS/TiO_2 composite photocatalysts.
2. High-temperature calcination of CdS/TiO_2 composite photocatalysts with different material ratios did not change the variation trend of their photocatalytic degradation efficiency, but the photocatalytic degradation efficiency increased slightly after calcination in general, which may be because of the reduction in adverse structural faults of CdS/TiO_2 composite photocatalyst after calcination.
3. The material ratio and ball milling process had an obvious influence on the photocatalytic degradation efficiency of CdS/TiO_2 composite photocatalysts when compared with high-temperature calcination. When the ball milling speed, time, and material ratio were 400 rpm, 10 h, and 25:75, respectively, the CdS/TiO_2 composite photocatalysts obtained by calcining after ball milling had the strongest photocatalytic performance on MO.
4. The irradiation conditions also had a significant influence on the photocatalytic degradation efficiency of CdS/TiO_2 composite photocatalysts. The photocatalytic degradation efficiency of CdS/TiO_2 composite photocatalysts under UV irradiation was much higher than that under sunlight irradiation.
5. As for the application, it is suggested that the CdS/TiO_2 composite photocatalysts can be prepared under the optimum conditions of the ball milling process if it is used in the industry. Since high-temperature calcination has a relatively small effect on its photocatalytic performance, for the sake of economy and operability, this step is not performed unless it is particularly necessary.

Acknowledgments: The authors sincerely acknowledge the National Natural Science Foundation of China (No. 51778066) for its financial support for this work.

Conflict of interest: The authors declare no conflict of interest regarding the publication of this paper.

References

[1] Boretti A, Castelletto S, Al-Zubaidy S. Concentrating solar power tower technology: present status and outlook. Nonlinear Eng. 2019;8:10–31.
[2] Shang Y, Zhong CW, Jia RN, Xiong HJ, Li H, Li XY, et al. Preparation of low-permittivity $K_2O–B_2O_3–SiO_2–Al_2O_3$ composites without the addition of glass. Nanotechnol Rev. 2019;8:459–66.
[3] Daghrir R, Drogui P, Robert D. Modified TiO_2 for environmental photocatalytic applications: a review. Ind Eng Chem Res. 2013;52:3581–99.
[4] Yi ZG, Tang Q, Jiang T, Cheng Y. Adsorption performance of hydrophobic/hydrophilic silica aerogel for low concentration organic pollutant in aqueous. Nanotechnol Rev. 2019;8:266–74.
[5] Xie Y, Wei W, Meng FB, Qu X, Li JY, Wang L, et al. Electric-field assisted growth and mechanical bactericidal performance of

ZnO nanoarrays with gradient morphologies. Nanotechnol Rev. 2019;8:315–26.
[6] Amade R, Heitjans P, Indris S, Finger M, Haeger A, Hesse D. Defect formation during high-energy ball milling in TiO_2 and its relation to the photocatalytic activity. J Photochem Photobiol A. 2009;207:231–5.
[7] Ismail AA, Bahnemann DW. Mesoporous titania photocatalysts: preparation, characterization and reaction mechanisms. J Mater Chem. 2011;21:11686–707.
[8] San N, Hatipoğlu A, Koçtürk G, Çınar Z. Photocatalytic degradation of 4-nitrophenol in aqueous TiO_2 suspensions: theoretical prediction of the intermediates. J Photochem Photobiol A. 2002;146:189–97.
[9] Fujishima A, Zhang XT, Tryk DA. Titanium dioxide photocatalysis: present situation and future approaches. C R Chim. 2006;9:750–60.
[10] Hoffmann MR, Martin ST, Choi W, Detlef WB. Environmental applications of semiconductor photocatalysis. Chem Rev. 1995;95:69–96.
[11] Asahi R, Morikawa T, Ohwaki T, Aoki K, Taga Y. Visible-light photocatalysis in nitrogen-doped titanium oxides. Science. 2001;293:269–71.
[12] Boufi S, Bouattour S, Ferraria AM, Chehimi MM, Vilar MR. Cotton fibres functionalized with plasmonic nanoparticles to promote the destruction of harmful molecules. Nanotechnol Rev. 2019;8:671–80.
[13] Pan XY, Yang MQ, Fu XZ, Zhang N, Xu YJ. Defective TiO_2 with oxygen vacancies: synthesis, properties and photocatalytic applications. Nanoscale. 2013;3601–14.
[14] Guo Z, Huang CX, Chen Y. Experimental study on photocatalytic degradation efficiency of mixed crystal nano-TiO_2 concrete. Nanotechnol Rev. 2020;9:219–29.
[15] Fujishima A, Zhang XT, Tryk DA. TiO_2 photocatalysis and related surface phenomena. Surf Sci Rep. 2008;63:515–82.
[16] Shi L, Benetti D, Li FY, Wei Q, Rosei F. Phase-junction design of MOF-derived TiO_2 photoanodes sensitized with quantum dots for efficient hydrogen generation. Appl Catal B Enviorn. 2020;263:10.
[17] Markowska-Szczupak A, Ulfig K, Morawski AW. The application of titanium dioxide for deactivation of bioparticulates: an overview. Catal Today. 2011;169:249–57.
[18] Liu WW, Liu MQ, Zhu YF, Gao Q. Photocatalytic dye degradation by TiO_2 nanocups synthesized via microwave-assisted solvothermal method. Nanosci Nanotechnol Lett. 2017;9:1579–83.
[19] Wang MX, Gao Q, Duan H, Ge MQ. Scalable synthesis of high-purity TiO_2 whiskers via ion exchange method enables versatile applications. RSC Adv. 2019;9:23735–43.
[20] Maruthapandi M, Eswaran L, Luong JHT, Gedanken A. Sonochemical preparation of polyaniline@TiO_2 and polyaniline@SiO_2 for the removal of anionic and cationic dyes. Ultrason Sonochem. 2020;62:8.
[21] Zangeneh H, Zinatizadeh AA, Zinadini S. Self-cleaning properties of L-histidine doped TiO_2–CdS/PES nanocomposite membrane: fabrication, characterization and performance. Sep Purif Technol. 2020;240:12.
[22] Rangkooy HA, Jahani F, Ahangar AS. Photocatalytic removal of xylene as a pollutant in the air using ZnO-activated carbon, TiO_2-activated carbon, and TiO_2/ZnO-activated carbon nanocomposites. Environ Eng Manage J. 2020;7:41–7.
[23] Ochiai T, Fujishima A. Photoelectrochemical properties of TiO_2 photocatalyst and its applications for environmental purification. J Photochem Photobiol C. 2012;13:247–62.
[24] Rambabu Y, Swati D, Manu J, Somnath Chanda R. High photoelectrochemical performance of reduced graphene oxide wrapped, CdS functionalized, TiO_2 multi-leg nanotubes. Nanotechnology. 2020. doi: 10.1088/1361-6528/ab84a0.
[25] She HD, Ma X, Chen KY, Liu H, Huang JW, Wang L, et al. Photocatalytic H-2 production activity of TiO_2 modified by inexpensive Cu(OH)(2) cocatalyst. J Alloys Compd. 2020;821:8.
[26] Qin YY, Li H, Lu J, Meng FY, Ma CC, Yan YS, et al. Nitrogen-doped hydrogenated TiO_2 modified with CdS nanorods with enhanced optical absorption, charge separation and photocatalytic hydrogen evolution. Chem Eng J. 2020;384:9.
[27] Chen SF, Chen L, Gao S. The preparation of coupled SnO_2/TiO_2 photocatalyst by ball milling. Mater Chem Phys. 2006;98:116–20.
[28] Chen XB, Clemens B. The electronic origin of the visible-light absorption properties of C-, N- and S-doped TiO_2 nanomaterials. J Am Chem Soc. 2008;130:5018–9.
[29] Ramana Reddy JV, Sugunamma V, Sandeep N, Hidaka H. Simultaneous impacts of Joule heating and variable heat source/sink on MHD 3D flow of Carreau-nanoliquids with temperature dependent viscosity. Nonlinear Eng. 2019;8:356–67.
[30] Anandan S, Ikuma Y, Niwa K. An overview of semi-conductor photocatalysis: modification of TiO_2 nanomaterials. Solid State Phenom. 2010;937:239–60.
[31] Trejo-Tzab R, Alvarado-Gil JJ, Quintana P, Bartolo-Pérez P. N-doped TiO_2 P25/Cu powder obtained using nitrogen (N_2) gas plasma. Catal Today. 2012;193:179–85.
[32] Tokmakci T, Ozturk A, Park J. Boron and zirconium co-doped TiO_2 powders prepared through mechanical ball milling. Ceram Int. 2013;39:5893–9.
[33] Jalalah M, Faisal M, Bouzid B, Ismail AA, Al-Sayari SA. Dielectric and photocatalytic properties of sulfur doped TiO_2 nanoparticles prepared by ball milling. Mater Res Bull. 2013;48:3351–6.
[34] Petrovic S, Rozic L, Grbic B, Radic N, Stefanov P, Stojadinovic S, et al. Effect of high energy ball milling on the physicochemical properties of TiO_2–CeO_2 mixed oxide and its photocatalytic behavior in the oxidation reaction. React Kinet Mech Catal. 2019;127:175–86.
[35] Aysin B, Ozturk A, Park J. Silver-loaded TiO_2 powders prepared through mechanical ball milling. Ceram Int. 2013;39:7119–26.
[36] Chen SF, Zhang SJ, Zhao W, Liu W. Study on the photocatalytic activity of TiN/TiO_2 nanoparticle formed by ball milling. J Nanopart Res. 2009;11:931–8.
[37] Balakrishnan M, John R. Properties of sol–gel synthesized multiphase TiO_2(AB)–ZnO(ZW) semiconductor nanostructure: an effective catalyst for methylene blue dye degradation. J Catal. 2020;10:1–16.
[38] Habib MA, Shahadat TM, Bahadur NM, Ismail IM, Mahmood AJ. Synthesis and characterization of ZnO–TiO_2 nanocomposites and their application as photocatalysts. Int Nano Lett. 2013;3:1–8.
[39] Zhou JW, Chu LL, Wang CB, Huang JX. Synthesis and photocatalytic properties of CdS/TiO_2 nano-composite by mechanochemistry method. J Synth Cryst. 2015;44:2590–6. (In Chinese).